International Journal of Materials and Chemistry 2020, 10(3): 31-43
DOI: 10.5923/j.ijmc.20201003.01

Copper Corrosion Inhibition in 1M HNO_3 by Loratadine: A Combined Experimental and Theoretical Study

Amadou Kouyaté[1,*], Mougo André Tigori[1], Dagri Cyrille Assouma[2], Dubois Rosemond Kacou[1], Paulin Marius Niamien[3], Bini Kouamé Dongui[1], Albert Trokourey[3]

[1]Laboratoire des Sciences et Technologies de l'Environnement, UFR Environnement, Université Jean Lorougnon Guédé, Daloa, Côte d'Ivoire
[2]UFR Sciences Biologiques, Université Péléforo Gon Coulibaly, Korhogo, Côte d'Ivoire
[3]Laboratoire de Constitution et de Réaction de la Matière, UFR SSMT, Université Félix Houphouët-Boigny, Abidjan, Côte d'Ivoire

Abstract Due to its massive use, the copper behavior in 1M nitric acid solution was studied in depth in this work. This study, which is mainly focused on loratadine inhibition properties, was carried out using mass loss technique at 298-323K and theoretical methods based on density functional theory (DFT) and Quantitative structure-property relationship (QSPR). Loratadine showed an inhibition efficiency of 85.07% at the concentration of 5.2210^{-4}M and the inhibition efficiency was found to be concentration and temperature dependent. Studies of adsorption isotherms have revealed that the molecule adsorbs to the copper surface according to the modified Langmuir isotherm or villamil isotherm. Adejo-Ekwenchi isotherm indicates that the adsorption of loratadine is dominated by chemisorption. The thermodynamic adsorption and activation parameters were also determined and discussed. Quantum chemistry calculations at the level of B3LYP/6-31G (d) verified any correlation between inhibition efficiency and molecular structure. QSPR model was used to establish a relationship between the quantum chemical parameters and the inhibition efficiency. The theoretical results are consistent with the experimental data reported.

Keywords Copper, Inhibition property, Loratadine, Mass loss technique, Density functional theory, Quantitative structure-property relationship

1. Introduction

Copper is widely used as a material in many fields, especially in industry because of its remarkable physical, mechanical, anticorrosion and biological properties [1]. During its use in acidic environments, this metal undergoes corrosion phenomenon. Indeed, the prediction of the long-term behavior of metallic structures, that means the evaluation of the damage which are likely to undergo over time under corrosion action, represents an important challenge, particularly on the economic and scientific levels. The knowledge of the corrosion rate of the metal in a given environment allows the development of a good strategy to monitor its dissolution in order to fight more efficiently against the degradation of materials by choosing the most appropriate protection method [2-5]. In terms of corrosion protection, it is possible to act on several levels. First on the material itself (judicious choice, adapted forms, constraints according to the applications...). Then on the material surface (coating, painting, any type of surface treatment etc.). Finally, on the environment with which the material is in contact (corrosion inhibitors). Currently, several researches are oriented towards at the use of corrosion inhibitors [2-5]. However, the rigid rules on environmental protection recommend the use of inhibitors that are very little toxic, eco-friendly and biodegradable [11-13]. In the course of this work, we made the choice to use loratadine which is a therapeutic molecule (antihistamine) and which meets well the requirements of the new international guidelines on environmental protection. Moreover, it contains heteroatoms (O and N) and bonds (π) that can offer special active electrons or vacant orbitals capable of accepting or giving electrons [14,15].

In recent years, the development of reliable computing tools coupled with the growth in computing power has enabled the implementation of molecular modeling techniques. That is why several works have used quantum chemical methods to explain the metals corrosion inhibition by organic compounds in acidic media [16-22]. These methods, which are generally based on the density functional theory (DFT), contribute largely to the search for effective inhibitors. These theoretical methods, which are less expensive than experimental methods, allow to clearly

* Corresponding author:
amadoukyte@yahoo.fr (Amadou Kouyaté)
Received: Nov. 21, 2020; Accepted: Dec. 8, 2020; Published: Dec. 22, 2020
Published online at http://journal.sapub.org/ijmc

explain the metal-inhibitor interactions while contributing to a better understanding of the inhibition properties of the studied molecule. Finally, the application of a Quantitative structure-property relationship (QSPR) predictive model in this study will lead to finding a relationship between inhibition efficiency and quantum chemical parameters [23,24].

The aim of the present work is to study the copper corrosion inhibition in nitric acid medium by 4-(8-chloro-5,6-dihydro-11Hbenzo [5,6] cyclohepta [1,2-b] pyridin-11-ylidene)-1-piperidinecarboxylic acid ethyl ester or loratadine from thermodynamic quantities of adsorption and activation and theoretical descriptor parameters such as the energy of the highest occupied molecular orbital (E_{HOMO}), the energy of lowest unoccupied molecular orbital (E_{LUMO}), the energy gap (ΔE) between E_{LUMO} and E_{HOMO}, the dipole moment (μ), the ionization energy (I), the electron affinity (A), the electronegativity (χ), the hardness (η), the softness (σ), the electrophylicity index (ω), the fraction of electron transferred (ΔN), total energy (E_T) are determined and analyzed. The local reactivity has been analyzed through Fukui function f_k^+ or f_k^- and dual descriptor (Δf_k^+ or Δf_k^-), since they indicate the reactive regions in the form of nucleophilic and electrophilic behavior of each atom in the molecule.

2. Experimental Details

2.1. Materials and Sample Preparation

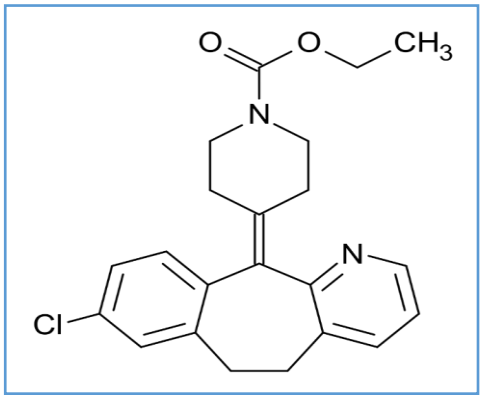

Figure 1. Molecular structure of Loratadine (LTD)

The inhibitor tested in this work namely loratadine or 4-(8-chloro-5,6-dihydro-11H-benzo [5,6] cyclohepta [1,2-b] pyridin-11-ylidene)-1-piperidine ethyl carboxylate. Analytical grade loratadine was purchased from Sigma Aldrich chemicals and solutions of the following concentrations: 0.0261mM; 0.156mM; 0.210mM and 0.522mM were prepared. The molecular structure is shown in Figure 1. The copper samples of 99.6% purity were in the form of a rod measuring 10 mm in length and 2 mm in diameter. These samples were successively polished with metallographic emery paper with grain sizes ranging from 150 to 600, rinsed with distilled water, degreased with acetone, rinsed again with distilled water and dried in a proofer from MEMMERT at 80°C for 20 min. This pre-treatment is intended to remove all traces of grease and native oxide before use. Analytical grade 70% nitric acid solution from Merck was used to prepare the corrosive aqueous solution. The solution was prepared by dilution of the commercial nitric acid solution using double distilled water. The blank was a 1M HNO_3 solution.

2.2. Masse Loss Technique

The mass (m_0) of each treated sample is determined using a precision balance from KERN, before immersion in 50mL of the corrosive 1M nitric acid solution prepared with or without inhibitor. After one hour of immersion at a constant temperature in a thermostat water bath from MEMMERT, each sample is removed from the solution, rinsed thoroughly with distilled water, dried and then re-weighed (m_1) with the balance to calculate the loss in mass ($\Delta m=m_0-m_1$). The different temperatures set during the experiment range from 298K to 323K.

2.3. Theoretical Methods

2.3.1. Quantum Chemical Calculations

In order to explain the most important electronic effects manifested by loratadine in copper corrosion inhibition, we have calculated the quantum chemical parameters. All calculations were performed in gas phase using Gaussian 09 software [25]. By improvement of computational method, density functional theory (DFT) has been widely used due to its accuracy and low computational cost to compute a wide variety of molecular properties and has provided reliable results that are consistent with experimental data [26]. The molecular configuration of the inhibitor was geometrically optimized by this theory (DFT) with the functional B3LYP [27] (Becke's three-parameter with Lee–Yang–Parr hybrid correlation functional) on 6-31 G (d) basis set.

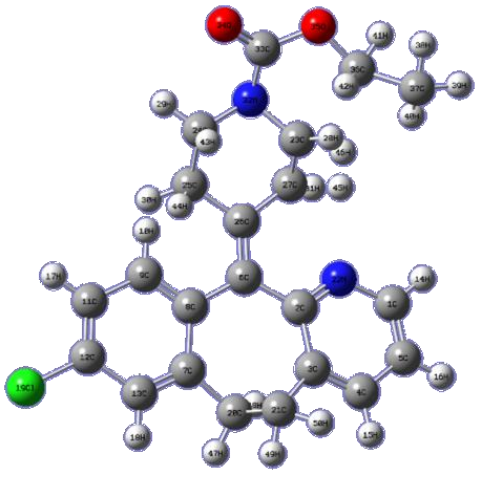

Figure 2. Optimized Structure of loratadine calculated by B3LYP/6-31G (d)

2.3.2. Quantitative Structure-Property Relationship Approach

QSPR approach is used to find a better relationship between experimental inhibition efficiency and theoretical molecular parameters. Moreover the objective of this method is to provide reliable theoretical tools capable of guiding researchers in the conduct of experiments for the discovery of new eco-friendly corrosion inhibitors [28].

For correlating some sets of parameters with the experimental data, a non-linear model was used [28]. This correlation is given by following expression:

$$IE(\%) = \frac{(Ax_j + B)C_i}{1+(Ax_j + B)C_i} \times 100 \quad (1)$$

Where A and B are real constants, determined by solving the system of simultaneous equations obtained from different values of inhibitor concentration C_i. In equation (1), a quantum chemical parameter is represented by x_j.

This approach may be validated by statistical indicators whose expressions are as follows:

The Sum of Square Errors (SSE):

$$SSE = \sum_{i=1}^{N} \left(IE_{\exp} - IE_{calc} \right)^2 \quad (2)$$

The Root Mean Square Error (RMSE):

$$RMSE = \sqrt{\frac{\sum_{i=1}^{N} \left(IE_{\exp} - IE_{calc} \right)^2}{N}} \quad (3)$$

3. Results and Discussion

3.1. Mass Loss Consideration

The corrosion rates (W), the degree of surface coverage (θ) and the inhibition efficiency IE (%) were calculated using the following expressions.

$$W = \frac{m_0 - m_1}{St} \quad (4)$$

$$\theta = \frac{W_0 - W}{W_0} \quad (5)$$

$$IE(\%) = \frac{W_0 - W}{W_0} \times 100 \quad (6)$$

Where m_0 is the mass of the sample before the test, m_1 is the mass of the sample after corrosion, S is the total area of the sample; t is the corrosion time and W the corrosion rate.

Where W_0, and W, are respectively the corrosion rate of the sample in the blank and in the blank containing loratadine.

Figure 3 gives respectively the evolution of the corrosion rate with concentration and temperature. Examination of Figure 3 shows that the corrosion rate increases with temperature for all concentrations. It can be seen that, regardless of temperature, the corrosion rate decreases as the concentration of the inhibitor increases. In the absence of inhibitor, the corrosion rate is very high, which shows that the addition of loratadine to the corrosive medium delays copper corrosion. In addition, the presence of loratadine promotes the creation of a protective layer that prevents copper from losing enough electrons or undergoing strong dissolution in acid. These results reveal that the studied molecule has a good inhibition performance against copper corrosion in nitric acid solution.

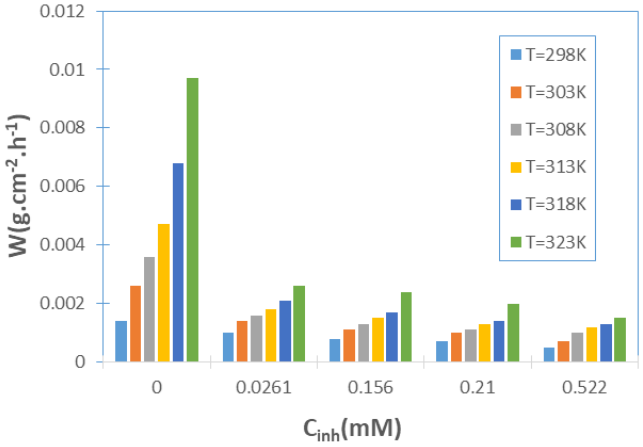

Figure 3. Evolution of the corrosion rate as a function of loratadine concentration for different temperatures

Analysis of the figure 4 reveals that the inhibition efficiency increases with temperature over the entire concentration range. For a given temperature, the inhibition efficiency increases with increasing concentration. All these observations show that loratadine acts as an effective inhibitor of copper corrosion in the concentration range studied. This behaviour could be explained by the formation of a physical barrier that separates copper from the nitric acid solution. Indeed, when the temperature rises, loratadine binds to the copper surface reducing its dissolution. This fixation or adsorption becomes important when the concentration of loratadine increases.

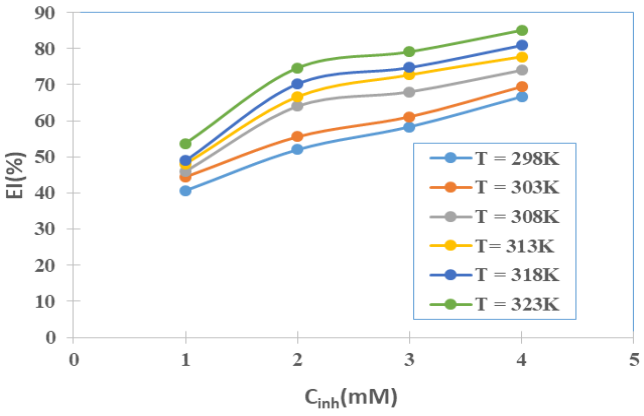

Figure 4. Inhibition efficiency versus concentration for different temperatures

3.2. Adsorption Isotherm and Thermodynamic Adsorption Parameters Study

The adsorption isotherms study involved in the process of metals corrosion inhibition by organic molecules allows

to show how these compounds bind to the surface of a metal. Indeed The adsorption of an organic adsorbate onto metal–solution interface can be represented by a substitutional adsorption process between the organic molecules in the aqueous solution phase ($Org_{(sol)}$) and the water molecules on the metallic surface ($H_2O_{(ads)}$) according to the equation [30]:

$$Org_{(sol)} + xH_2O_{(ads)} \rightleftarrows Org_{(ads)} + xH_2O_{(sol)} \quad (7)$$

Where $Org_{(sol)}$ and $Org_{(ads)}$ are respectively the organic species dissolved in the aqueous solution and adsorbed onto the metallic surface. $H_2O_{(sol)}$ and $H_2O_{(ads)}$ are respectively the water molecule in the bulk solution and that adsorbed onto the metallic surface; x is the size ratio representing the number of water molecules replaced by one organic adsorbate.

In this work we attempted various adsorption isotherms and selected those that better reflect loratadine behavior on copper surface. So we have retained Langmuir, Temkin, El-awady and Freundlich isotherms. The equations that define these isotherms are expressed in Table 1.

Table 1. Equation of studied isotherms

Isotherm	Equations
Langmuir	$\frac{C_{inh}}{\theta} = \frac{1}{K_{ads}} + C_{inh}$
Temkin	$\theta = \frac{2.303}{f}[logK_{ads} + logC_{inh}]$
El-Awady	$log\left(\frac{\theta}{1-\theta}\right) = logK' + ylogC_{inh}$
Freundlich	$log\theta = logK_{ads} + nlogC_{inh}$

C_{inh} is loratadine's concentration;
K_{ads} is the equilibrium constant of the adsorption process,
f is a factor of energetic inhomogeneity in the surface;
θ is is surface coverage;
$K_{ads}=K'^{1/y}$;
1⁄y is active sites occupied by an inhibitor molecule.

Figures 5, 6, 7 and 8 show the representation of these different isotherms.

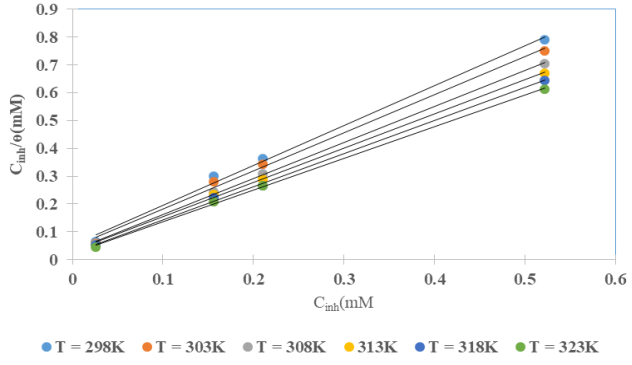

Figure 5. Langmuir adsorption isotherm plots of LTD on copper in 1M HNO_3

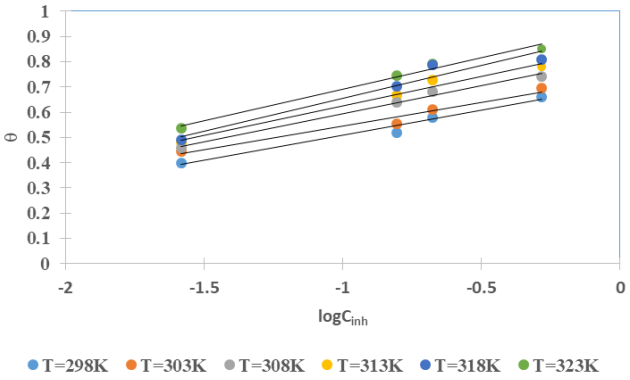

Figure 6. Temkin adsorption isotherm plots of LTD on copper in 1M HNO_3

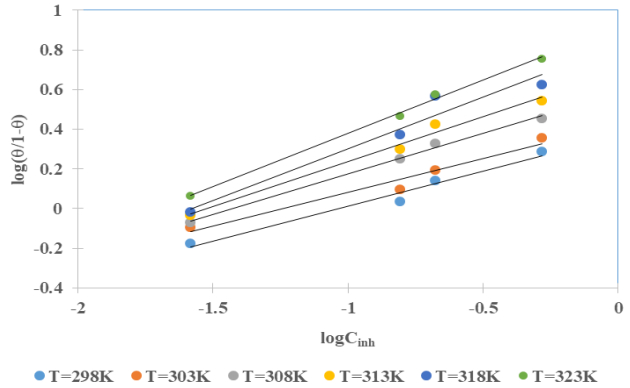

Figure 7. El-Awady adsorption isotherm plots of LTD on copper in 1M HNO_3

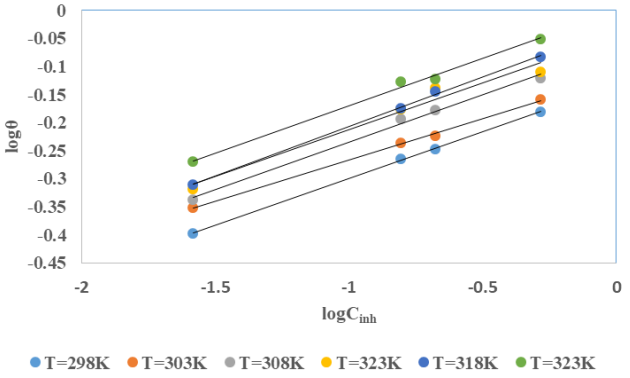

Figure 8. Freundlich adsorption isotherm plots of LTD on copper in 1M HNO_3

All the tested isotherms yield straight lines as shown in Figures 5, 6, 7 and 8. Table 2 gives the different parameters of studied isotherms.

By looking the table 2, it is clear that the correlation coefficients of Langmuir isotherm are closer to unity than the other isotherms. Thus, this isotherm better reflects loratadine behavior with respect to copper corrosion in 1M HNO_3. Nevertheless, Temkin and El-Awady models can be applied. For Temkin model [31], the parameter f (where 2.303/f is the slope of straight lines) having a positive value, there would be repulsion forces between the molecules adsorbed on copper. As for El-Awady model [32], the inverse of the

slopes (1/y) of the straight lines obtained is greater than unity, this means that a Loratadine molecule occupies more than one site. Langmuir adsorption model requires that the interactions between adsorbed particles are negligible and that each site can adsorb only one particle [33]. In this case, loratadine adsorption on copper is not rigorously done according to Langmuir model; it is done according to the modified Langmuir isotherm or Villamil model [34]. This model represented by the equation:

Table 2. Isotherms parameters for various temperatures

Isotherm	T(K)	R^2	Slope	Intercept
Langmuir	298	0.995	1.435	0.0516
	303	0.995	1.3715	0.0452
	308	0.999	1.2971	0.0322
	313	0.999	1.2330	0.3040
	318	0.999	1.1878	0.0255
	323	0.999	1.1383	0.0223
Temkin	298	0.975	0.1984	0.7062
	303	0.969	0.1886	0.7346
	308	0.991	0.2202	0.8144
	313	0.976	0.2354	0.8603
	318	0.943	0.2596	0.9142
	323	0.984	0.2480	0.9391
El-Awady	298	0.973	0.3532	0.3676
	303	0.963	0.3502	0.4236
	308	0.996	0.4087	0.5828
	313	0.9851	0.4531	0.6888
	318	0.947	0.5129	0.8224
	323	0.996	0.5364	0.9161
Freundlich	298	0.999	0.1673	-0.1321
	303	0.998	0.1469	-0.1191
	308	0.994	0.1684	-0.0662
	313	0.969	0.1671	-0.0452
	318	0.994	0.1766	-0.0297
	323	0.994	0.1683	0.0012
	323	0.994	2.2191	2.0472

$$\frac{C_{inh}}{\theta} = \frac{n}{K_{ads}} + nC_{inh} \quad (8)$$

The knowledge of the suitable adsorption isotherm allows to determine the thermodynamic adsorption parameters. The change in free energy of adsorption (ΔG^0_{ads}) is calculated using the following relation [35]:

$$\Delta G^0_{ads} = -RT\ln(55{,}5\ K_{ads}) \quad (9)$$

Where R is the perfect gas constant, T is absolute temperature and the constant 55.5 is the molar concentration of water. K_{ads} is the equilibrium constant of the adsorption process. The values of Adsorption equilibrium constant are deduced from the parameters of the modified Langmuir isotherm (intercept of straight lines).

With regard to the other thermodyamic adsorption parameters (adsorption enthalpy ΔH^0_{ads} and adsorption entropy ΔS^0_{ads}, they are calculated using the following relationship:

$$\Delta G^0_{ads} = \Delta H^0_{ads} - T\Delta S^0_{ads} \quad (10)$$

The representation of ΔG^0_{ads} as a function of temperature (figure 9) leads to the values of ΔH^0_{ads} (intercept of straight lines) and ΔS^0_{ads}, (the slope of the straight line). The different thermodynamic adsorption parameters are recorded in table 3.

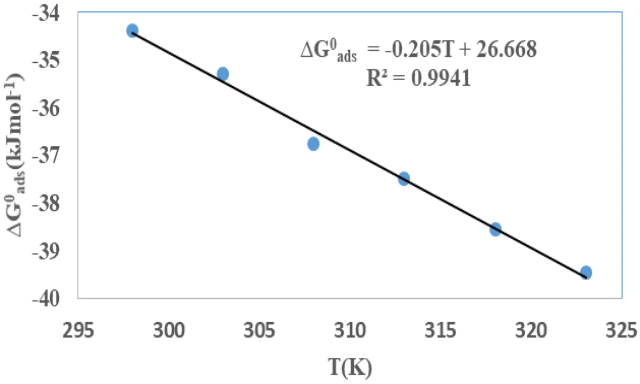

Figure 9. ΔG^0_{ads} versus Temperature

Table 3. K_{ads} and thermodynamic adsorption parameters for LTD

T(K)	$K_{ads}(M^{-1})$	$\Delta G^0_{ads}\,(kJ.mol^{-1})$	$\Delta H^0_{ads}\,(kJ.mol^{-1})$	$\Delta S^0_{ads}\,(J.mol^{-1}.K^{-1})$
298	19380	-34.393	26.668	205
303	22124	-35.303		
308	31056	-36.754		
313	32895	-37.500		
318	39216	-38.564		
323	43668	-39.459		

The negative values of ΔG^0_{ads} indicate the stability of the adsorbed layer on copper surface and the spontaneity of the adsorption process [36]. These values become more and more negative as the temperature rises, reflecting the strengthening of metal-molecule interactions. This reinforcement of interactions could justify the high values of inhibition efficiency obtained experimentally at high temperature. An increase in the equilibrium constant K_{ads} is also observed when the temperature rises, reflecting the fact that the rise in temperature easily favours the inhibitor

adsorption on copper surface. The prediction of adsorption type displayed by the inhibitor can be made by the magnitude ΔG^0_{ads}. In our case the values of ΔG^0_{ads} range from -38.46 KJ.mol^{-1} to 34.39 KJ.mol^{-1}, indicating a predominant chemisorption process [37,38]. The positive sign of ΔH^0_{ads} symbolize the endothermic character of loratadine adsorption on copper in nitric acid solution [39]. The positive values of ΔS^0_{ads} indicate that the disorder increases when loratadine adsorbs on the copper surface due to the desorption of water molecules [40].

In order to correctly justify the adsorption mode of the studied molecule, we have used Adejo–Ekwenchi isotherm [41]. Indeed, this isotherm allows us to know the adsorption mode of an organic compound. This model is based on the following equation. Figure 10 shows the representation of this isotherm

$$\log\left(\frac{1}{1-\theta}\right) = logK_{AE} + blogC_{inh} \quad (11)$$

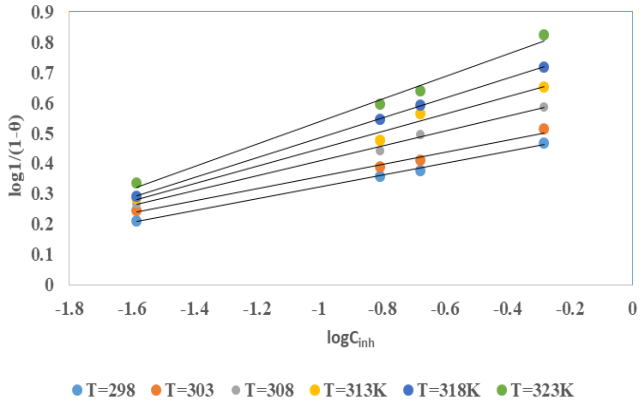

Figure 10. Adejo–Ekwenchi isotherm plots of LTD on copper in 1M HNO_3

The parameters for this isotherm are listed in Table 4

Table 4. Adejo–Ekwenchi isotherm parameters

T(K)	R^2	b	logK_{AE}	K_{AE}
298	0.996	0.1946	0.517	3.289
303	0.989	0.2019	0.5589	3.622
308	0.996	0.2446	0.6527	4.495
313	0.983	0.286	0.7343	4.424
318	0.999	0.3281	0.8117	6.482
323	0.990	0.3699	0.909	8.111

As reflected in Table 4, parameters b and K_{AE} increase with temperature, showing that the adsorption of loratadine on copper is dominated by chemisorption [42].

3.3. Effect of Temperature and Activation Parameters of the Corrosion Process

The effect of temperature on corrosion and its inhibition process for copper in 1M HNO_3 in absence and presence of different concentrations of loratadine at different temperatures ranging from 298K to 323K was evaluated. The dependence of corrosion rate on the temperature can be regarded as an Arrhenius - type process, the rate of which is given by [43]:

$$logW = logA - \frac{E_a}{2{,}3R.T} \quad (12)$$

Where W is the corrosion rate in the presence of inhibitor, E_a the apparent activation energy, R the universal gas constant, A the frequency factor. The plot of logW versus 1/T for copper in the studied solution is given by the figure 11.

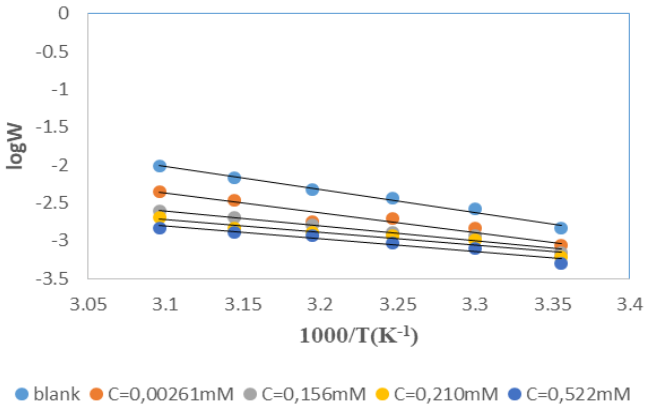

Figure 11. Arrhenius plots for copper in 1M HNO_3 without and with LTD

Arrhenius plots permit to deduce the values of the activation energies E_a using the slopes of the linear plots. All the obtained values are listed in table 5.

The temperature effect was also verified by determining the Changes in activation enthalpy ΔH^*_a and activation entropy ΔS^*_a using Eyring transition state equation.

$$W = \frac{R.T}{\aleph.h} exp\left(\frac{\Delta S^*_a}{R}\right).exp\left(-\frac{\Delta H^*_a}{R.T}\right) \quad (13)$$

This equation can be expressed as:

$$log\left(\frac{W}{T}\right) = log\left(\frac{R}{\aleph h}\right) + \frac{\Delta S^*_a}{2{,}303R} - \frac{\Delta H^*_a}{2{,}303RT} \quad (14)$$

Where h the Planck constant, $\aleph$ the Avogadro number

The transition state plots of $\log(\frac{W}{T})$ versus $\frac{1}{T}$ is given in Figure 12.

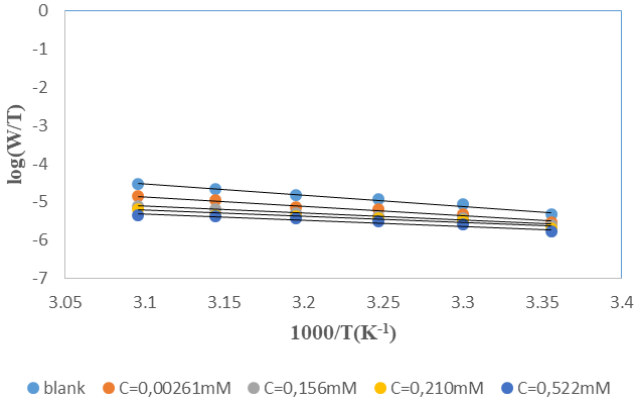

Figure 12. Arrhenius plots for copper corrosion in 1M HNO_3 in absence and presence of different concentrations of LTD

Table 5. Thermodynamic activation parameters of copper dissolution in 1M HNO_3 without and with LTD

Cinh (mM)	$E_a(kJmol^{-1})$	k_0(unité	$\Delta H_a^*(kJmol^{-1})$	$\Delta S_a^*(Jmol^{-1}K^{-1})$
0	58.003	$2.37X10^7$	55.992	-110.46
0.026	49.198	$3.91X10^5$	48.329	-140.56
0.156	37.598	$3.06X10^3$	35.051	-186.58
0.210	33.043	$4.34X10^2$	31.032	-201.10
0.522	32.559	$2.94X10^2$	30.549	-204.34

ΔH^*_a and ΔS^*_a were computed respectively from the slopes $(-\frac{\Delta H_a^*}{2{,}303RT})$ and intercepts $(log(\frac{R}{Nh}) + \frac{\Delta S_a^*}{2{,}303R})$ of the straight lines obtained. The obtained values are recorded in Table 5.

The apparent activation energy (E_a) values in presence of loratadine are lower than the value obtained without this molecule (Cinh = 0). These observations reveal that the inhibition of corrosion reactions is influenced by chemisorption [44]. E_a decreases when the concentration of inhibitor increases, favouring the Cu^{2+} ions formation and thus the formation of the Cu-Inh complex leading to the reduction of corrosion phenomenon at high temperature. Indeed, the inhibitor adsorbs on metal surface by chemical bonds which are strong (chemisorption) and resists at high temperature. These observations justify the good performance of the molecule when the temperature increases. The values from ΔH^*_a are positive and are increasingly lower in presence of loratadine. This reflects an endothermic dissolution process leading to a slow dissolution of copper in the solution studied [45]. The negative sign of ΔS^*_a implies that the disorder decreases from reactant to activated complex [46].

3.4. Quantum Chemistry Consideration

Table 6. Quantum chemical parameters of loratadine, calculated using B3LYP/6 - 31G (d)

Parameters	LTD
E_{HOMO} (eV)	-5.6660
E_{LUMO} (eV)	-1.6910
Energy gap ΔE (eV)	3.9750
Dipole moment $\mu(D)$	8.1898
Ionization energy $I(eV)$	5.6660
Electron affinity $A(eV)$	1.6910
Absolute electronegativity χ (eV)	3.6785
Hardness $\eta(eV)$	1.988
Softness $(\sigma(eV)^{-1}$	0.5031
Fraction of electron transferred ΔN	0.3274
Electrophylicity index ω	3.4041
Total energy $E_T(Ha)$	-1572.15

In this study the quantum chemical parameters have been calculated by using the conceptual DFT descriptors which are very important to explain the molecule reactivity. In general, this concept permits to confirm the experimental results. Their values are listed in table 6. So, the relationship between these parameters and inhibition efficiency was investigated.

The expressions used to determine the parameters listed in Table 6 are defined as follows [47-49]:

$$\Delta E = E_{LUMO} - E_{HOMO} \quad (15)$$

$$I = -E_{HOMO} \quad (16)$$

$$A = -E_{\mathrm{LUMO}} \quad (17)$$

$$\chi = -\mu_p = \left(\frac{\partial E}{\partial N}\right)_{v(r)} \quad (18)$$

$$\chi = \frac{I+A}{2} \quad (19)$$

$$\eta = \frac{I-A}{2} \quad (20)$$

$$\sigma = \frac{1}{\eta} = \frac{2}{I-A} \quad (21)$$

$$\Delta N = \frac{\phi_{cu} - \chi_i}{2(\eta_{cu} + \eta_i)} \quad (22)$$

$$\omega = \frac{\mu_P^2}{2\eta} = \frac{(I+A)^2}{4(I-A)} \quad (23)$$

Where ϕ_{cu} and χ_i denote respectively the absolute electronegativity of copper and the inhibitor, η_{cu} and η_i are respectively the global hardness of copper and the inhibitor. In this work ΔN has been determined using ϕ_{cu} = 4.98 eV [50] and η_{cu}= 0 [51], assuming that for a metallic bulk $I=A$ because they are softer than the neutral metallic atoms.

The higher energy of HOMO (E_{HOMO}) value, the greater is the tendency of the molecule to offer electrons to unoccupied orbital of the metal; in addition, the lower the energy of LUMO (E_{LUMO}), the higher is the affinity for accepting electrons from the metal surface [52]. The inhibition potential of a reacting organic compound can be evaluated by the orbital energy difference. Furthermore, the smaller of orbital energy difference between the interacting orbitals, i.e. HOMO and LUMO ($\Delta E = E_{LUMO} - E_{HOMO}$) would promote strong metal-molecule interaction [53]. In our case, the high value of E_{HOMO} (-5.6660eV) and the low values of E_{LUMO} (-1.6910eV) and ΔE (3.9750eV) of loratadine justify the high inhibition efficiency values obtained experimentally.

Global hardness (η) and softness (σ) are related to inhibition efficiency which also depend on the energy gap. In fact a good inhibitor has a high softness value and a low hardness value [54,55]. Loratadine has a low hardness value (η = 1.988 eV) and a high softness value [σ = 0.5031 $(eV)^{-1}$] is expected to have a high inhibition efficiency. These values

are in agreement with the experimental results.

The absolute electronegativity (χ) is the chemical property that describes the ability of a molecule to attract electron towards itself in a covalent bond [50]. The electronegativity value of loratadine is lower than copper, which confirms the electrons movement from loratadine to copper.

For dipole moment (μ), several authors state that the inhibition efficiency increases with increasing values of this parameter [56,57]. Moreover, survey of the literature reveals that several irregularities appeared in case of correlation of dipole moment with inhibitor efficiency [58,59]. So in general, there is no significant relationship between the dipole moment values and inhibition efficiencies.

The fraction of electrons transferred (ΔN) of a molecule reflects its ability to give electrons. According to Lukovits' study, if $\Delta N < 3.6$ then the efficiency of inhibition increases with the molecule's ability to give electrons to the metal [59]. In our work $\Delta N < 3.6$, which shows that loratadine has a good inhibition performance in electron donation.

The electrophilicity index (ω) measures the propensity of chemical species to accept electrons. A high value of (ω) [49] describes a good electrophile, while a low value of (ω) describes a good nucleophile. In our case, the electrophilicity index of the molecule is high, expressing that loratadine is a good electrophile.

Loratadine has negative value of total energy ($E_T < 0$) and positive value of hardness ($\eta > 0$), which proves that the charge transfer from each molecule to the metal is energetically favorable [60]. So, there is a strong interaction between the molecules and the copper surface.

Local reactivity was analyzed by means of Fukui indices and dual descriptor in order to assess the nucleophilic and electrophilic attack centre.

The Fukui [61,62] functions expressed using the limit difference approximation is given as follows

For nucleophilic attack

$$f_k^+ = [q_k(N+1) - q_k(N)] \quad (24)$$

For electrophilic attack)

$$f_k^- = [q_k(N) - q_k(N-1)] \quad (25)$$

Where $q_k(N+1)$, N and $q_k(N-1)$ are the electronic population of atom k in $(N+1)$, N and $N-1$ electrons systems.

The dual descriptor [63,64] is used to locate nucleophilic and electrophilic sites of attack with all possible precision. It is defined by the following expression

$$\Delta f_k(\mathrm{r}) = f_k^+ - f_k^- \quad (26)$$

The nucleophilic attack and electrophilic attack are given respectively by the highest and the lowest value of $\Delta f_k(\mathrm{r})$.

All the local parameters are collected in Table 7.

It is clear from the analysis in Table 7 that N(22) with the high value of $\Delta f_k(\mathrm{r})$ and f_k^+ is the most probable nucleophilic attack site while C(33) with the maximum value of f_k^- and the lowest value of $\Delta f_k(\mathrm{r})$ is most probable electrophilic attack site.

The HOMO-LUMO diagrams are presenting by Figure 13.

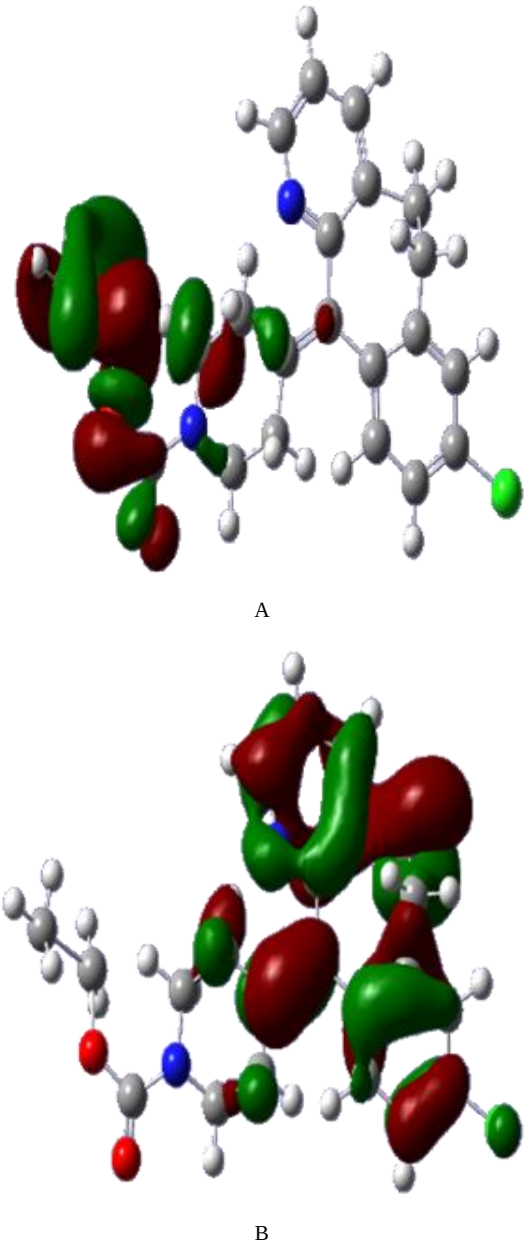

A

B

Figure 13. HOMO (A) and LUMO (B) orbitals of by B3LYP/6-31G (d)

3.5. Quantitative Structure-Property Relationship (QSPR) Assessment

In order to select a set of relevant quantum chemical parameters capable of finding a relationship between these parameters and experimental inhibition efficiencies, QSPR method was used. For this method, we used inhibition efficiencies at 298K in the same concentration range.

The constants determined for the sets of parameters are recorded in the table 8.

The Theoretical versus experimental efficiencies of LTD for different sets are represented in Figures 14.

Table 7. Calculated Mulliken atomic charges, Fukui functions and dual descriptor by DFT B3YLP6-31/ G (d)

Atom N°	$q_k(N+1)$	$q_k(N)$	$q_k(N-1)$	f_k^+	f_k^-	Δf_k(r)
1 C	0.003745	0.026275	-0.007247	-0.02253	0.033522	-0.056052
2 C	0.002679	0.282502	0.000196	-0.279823	0.282306	-0.562129
3 C	-0.008461	-0.02058	0.001289	0.012119	-0.021869	0.033988
4 C	0.006635	-0.184788	0.00108	0.191423	-0.185868	0.377291
5 C	-0.004369	-0.131138	0.013507	0.126769	-0.144645	0.271414
6 C	-0.01177	0.063734	0.032178	-0.075504	0.031556	-0.10706
7 C	0.001989	0.232612	0.007232	-0.230623	0.22538	-0.456003
8 C	0.002934	0.114453	-0.009328	-0.111519	0.123781	-0.2353
9 C	-0.006642	-0.188826	0.015887	0.182184	-0.204713	0.386897
10 H	0.000364	-0.021255	-0.000798	0.021619	-0.020457	0.042076
11 C	0.002271	-0.161522	-0.00541	0.163793	-0.156112	0.319905
12 C	-0.002773	-0.057349	0.012639	0.054576	-0.069988	0.124564
13 C	-0.002031	-0.220257	-0.006179	0.218226	-0.214078	0.432304
14 H	-0.000146	0.151953	0.000254	-0.152099	0.151699	-0.303798
15 H	-0.00031	0.14141	-0.000161	-0.14172	0.141571	-0.283291
16 H	0.000031	0.141108	-0.000708	-0.141077	0.141816	-0.282893
17 H	-0.000071	0.153145	0.000187	-0.153216	0.152958	-0.306174
18 H	0.000103	0.145566	0.000234	-0.145463	0.145332	-0.290795
19 Cl	-0.000441	0.017865	0.000374	-0.018306	0.017491	-0.035797
20 C	-0.002754	0.436864	0.001444	-0.439618	0.43542	-0.875038
21 C	-0.055879	-0.494088	0.001313	0.438209	-0.495401	0.93361
22 N	-0.008461	-0.524296	0.020398	**0.515835**	-0.544694	**1.060529**
23 C	-0.026158	-0.103261	-0.062305	0.077103	-0.040956	0.118059
24 C	-0.000152	-0.138598	-0.002268	0.138446	-0.13633	0.274776
25 C	-0.002883	-0.399519	0.001789	0.396636	-0.401308	0.797944
26 C	0.004788	0.048154	0.011088	-0.043366	0.037066	-0.080432
27 C	-0.027551	-0.02235	0.046287	-0.005201	-0.068637	0.063436
28 H	0.00262	0.180897	-0.007621	-0.178277	0.188518	-0.366795
29 H	0.000082	0.194109	-0.000229	-0.194027	0.194338	-0.388365
30 H	0.000341	0.249517	-0.000305	-0.249176	0.249822	-0.498998
31 H	0.000388	0.216198	0.000445	-0.21581	0.215753	-0.431563
32 N	-0.008258	-0.439756	0.016783	0.431498	-0.456539	0.888037
33 C	-0.000505	0.705978	-0.004619	-0.706483	**0.710597**	**-1.41708**
34 O	0.022458	-0.48855	0.000568	0.511008	-0.489118	1.000126
35 O	0.057675	-0.447804	0.059526	0.505479	-0.50733	1.012809
36 C	0.035209	-0.215306	0.347087	0.250515	-0.562393	0.812908
37 C	-0.000454	-0.081679	0.55412	-0.081225	-0.635799	0.717024
38 H	-0.06158	0.241781	-0.015268	-0.303361	0.257049	-0.56041
39 H	-0.020701	0.14662	-0.01502	-0.167321	0.16164	-0.328961
40 H	-0.012779	0.258506	-0.008916	-0.271285	0.267422	-0.538707
41 H	0.081322	0.125982	-0.022078	-0.04466	0.14806	-0.19272
42 H	0.023377	0.23451	0.008146	-0.211133	0.226364	-0,437497
43 H	-0.00074	0.178886	0.001424	-0.179626	0.177462	-0.357088
44 H	0.000028	0.264302	0.000784	-0.264274	0.263518	-0.527792
45 H	0.008581	0.079473	-0.010271	-0.070892	0.089744	-0.160636
46 H	-0.008066	0.082411	0.019195	-0.090477	0.063216	-0.153693
47 H	0.000101	0.171681	-0.000055	-0.17158	0.171736	-0.343316
48 H	0.001079	0.190737	-0.000062	-0.189658	0.190799	-0.380457

Atom N°	$q_k(N+1)$	$q_k(N)$	$q_k(N-1)$	f_k^+	f_k^-	Δf_k(r)
49 H	-0.002527	0.2863	0.001165	-0.288827	0.285135	-0.573962
50 H	-0.001633	0.266739	0.002226	-0.268372	0.264513	-0.532885

Table 8. Values of coefficients A, B, D, E, R^2 and Statistical parameters of the sets

Set of parameters	A	B	D	E	R^2	SSE	RMSE
(E_{HOMO}, ω, η)	$4.0995X10^{12}$	$6.8163X10^{12}$	-12025.8563	883.944738	0.9428	950.50	15.42
$(\Delta E, \mu, \sigma)$	592.630297	-487.879622	1348.83239	961.34131	**0.9709**	**680.71**	**13.05**
(χ, ω, E_{LUMO})	593.296664	272.879355	-614.463732	-4150.40112	0.9695	776.95	13.94
$(E_{HOMO}, E_{LUMO}, \mu)$	505.04886	-232.658638	202.4503	-2120.83134	0.9759	806.58	14.20

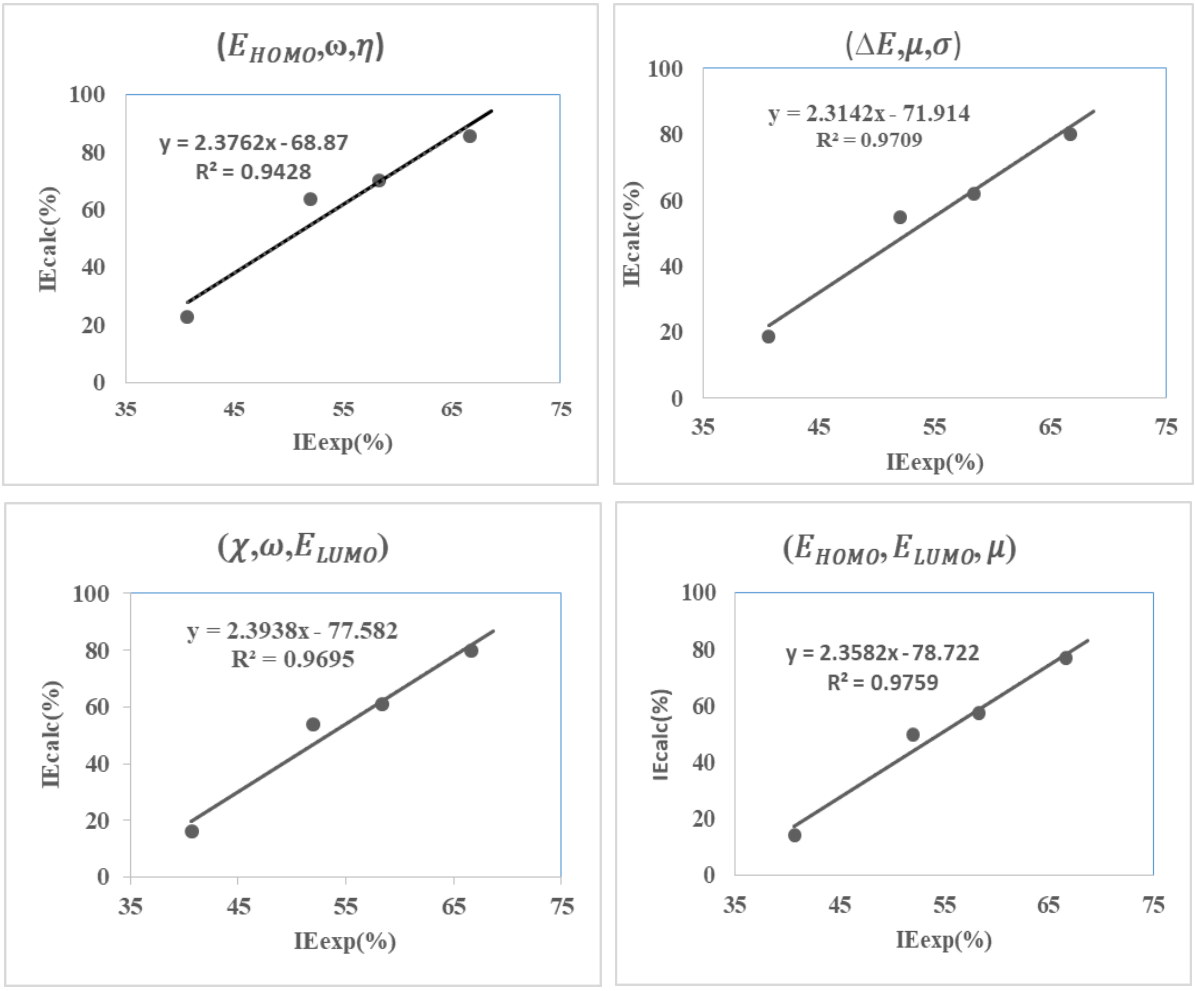

Figure 14. Theoretical versus experimental efficiencies of LTD for different sets of parameters

Referring to the data in the table 8, it appears that the set of parameter $(\Delta E, \mu, \sigma)$ with the lowest value of RMSE and correlation coefficient R^2=0.9709 is the best parameter to describe loratadine behavior of copper corrosion inhibition in 1M HNO_3.

4. Conclusions

Mass loss and theoretical method were used to evaluate the copper corrosion inhibition by loratadine in 1M HNO_3. The main finding of this study are as follows:

- Loratadine acts a good inhibitor for copper corrosion in 1M HNO_3 and its Inhibition efficiency increases with increasing concentration and temperature.
- The adsorption of loratadine on copper surface obeys the modified Langmuir adsorption isotherm or Villamil model and is a spontaneous, exothermic process accompanied by an increase in entropy.
- The adsorption process is dominated by chemisorption.
- Thermodynamic activation parameters indicate an exothermic dissolution process.
- The Fukui functions and the dual descriptor have

proved that N(22) and C(33) are respectively the probable sites of nucleophilic and electrophilic attack.

- $(\Delta E, \mu, \sigma)$ is the best set of parameters for correlating theoretical and experimental inhibitory efficiencies.
- Calculated theoretical parameters support the experimental results.

ACKNOWLEDGEMENTS

The authors gratefully acknowledged the support of the Environmental Science and Technology Laboratory, Daloa (Côte d'Ivoire).

REFERENCES

[1] Techno without borders, copper in all its states, Technology, 2008, 155, 8-13.

[2] Mendonca, G.L.F., Costa, S.N., Freire, V.N., Casciano, P.N.S., Correia, A.N., 2017, Lima-Neto, P.d. Understanding the corrosion inhibition of carbon steel and copper in sulphuric acid medium by amino acids using electrochemical techniques allied to molecular modelling methods, Corrosion Science, 115, 41–55.

[3] Zhang, D.Q., Cai, Q.-R., Gao, L.-X., Lee, K.Y., 2008, Effect of serine, threonine and glutamic acid on the corrosion of copper in aerated hydrochloric acid solution, Corrosion Science. 50(12), 3615–3621.

[4] Laggoun, R., Mahmoud F., Saidat, B., Benghia, A., Chaabani, A., 2020, Effect of p-toluenesulfonyl hydrazide on copper corrosion in hydrochloric acid solution. Corrosion Science 165, 108363.

[5] Talebian, M., Raeissi, K., Atapour, M., Fernández-Pérez, B.M., Salarvand, Z., Meghdadi, S., Amirnasr, M., Souto, R.M., 2018, Inhibitive effect of sodium (E)-4-(4-nitrobenzylideneamino) benzoate on the corrosion of some metals in sodium chloride solution. Applied Surface Science 447, 852-865.

[6] Qiang, Y., Zhang, S., Xu, S., Li, W., 2016, Experimental and theoretical studies on the corrosion inhibition of copper by two indazole derivatives in 3.0% NaCl solution, Journal of colloid and interface science, 472, 52-59.

[7] Wang, D., Xiang, B., Liang, Y., Song, S., Liu, C., 2014, Corrosion control of copper in 3.5wt.% NaCl Solution by Domperidone: Experimental and Theoretical Study, Corrosion Science 85,77-86.

[8] Saira, F., Renu, S., Faiza A., Ajar K., Amin, B., Heinz-Bernhard, K., 2019) Study of new amphiphiles based on ferrocene containing thioureas as efficient corrosion inhibitors: Gravimetric, electrochemical, SEM and DFT studies. Journal of Industrial and Engineering Chemistry 76, 374-387.

[9] Döner, A., Yüce, A.O., Kardaş, G., 2013, Inhibition Effect of Rhodanine-N-Acetic Acid on Copper Corrosion in Acidic Media, Industrial & Engineering Chemistry Research 52(29), 9709-9718.

[10] L. Gao, S. Peng, X. Huang, Z. Gong,2020, A combined experimental and theoretical study of papain as a biological eco-friendly inhibitor for copper corrosion in H2SO4 medium, Applied Surface Science, 511, 145446.

[11] Tigori, M.A., Bony, F. N., Niamien, P. M., Yapo, A. J., Trokourey, A., 2016, Experimental and theoretical studies on Riboflavin's behaviour against copper corrosion in 1M HNO3, Archives of Applied Science Research, 8 (5): 18-32.

[12] Singh, A.K., Mohapatra, S. and Pani, B., 2016, Corrosion Inhibition Effect of Aloe Vera gel: Gravimetric and Electrochemical Study. Journal of Industrial and Engineering Chemistry, 25, 288-297.

[13] Deyab, M.A., 2015, Egyptian Licorice Extract as a Green Corrosion Inhibitor for Copper in Hydrochloric Acid Solution. Journal of Industrial and Engineering Chemistry, 25, 384-389.

[14] Ahmed, R.A., 2016, Investigation of Corrosion Inhibition of Vitamins B1 and C on Mild Steel in 0.5 M HCl Solution: Experimental and Computational Approach. Oriental Journal of Chemistry, 32(1), 295-304.

[15] Fucks-Godec, R. and Zergav, G., 2015, Corrosion Resistance of High-Level Hydrophobic Layers Combination with Vitamin E-(α-tocopherol) as Green Inhibitor. Corrosion Science, 97, 7-16.

[16] Zohreh Parsaee, Pouya Haratipour, Milad Janghorban Lariche and Arash Vojood., 2018, A novel high performance nano chemosensor for copper (II) ion based on an ultrasound-assisted synthesized diphenylamine-based Schiff base: Design, fabrication and density functional theory calculations. Ultrasonics Sonochemistry, 41, 337-349.

[17] Elias, E., Elemike T., Henry, U., Nwankwo, D., Onwudiwe C, Hosten, E. C., 2017, Synthesis, crystal structures, quantum chemical studies and corrosion inhibition potentials of 4-(((4-ethylphenyl)imino)methyl)phenol and (E)-4-((naphthalen-2-ylimino)methyl)phenol Schiff bases. Journal of Molecular Structure, 1147, 252-265.

[18] L. Guo, W.P. Dong, S.T. Zhang, 2014, Theoretical challenges in understanding the inhibition mechanism of copper corrosion in acid media in the presence of three triazole derivatives, Royal Society of Chemistry Adv, 4, 41956-41967.

[19] Tigori, M.A., Kouyate, A., Kouakou, V., Niamien, P.M. and Trokourey, A., 2020, Inhibition Performance of Some Sulfonylurea on Copper Corrosion in Nitric Acid Solution Evaluated Theoretically by DFT Calculations, Open Journal of Physical Chemistry, 10(3), 139-157.

[20] I.B. Obot, D.D. Macdonald and Z.M. Gasem., 2015, Density functional theory (DFT) as a powerful tool for designing new organic corrosion inhibitors. Part 1: An overview. Corrosion Science 99, 1-30.

[21] H. Elmsellem, T. Harit, A. Aouniti, F. Malek, A. Riahi, A. Chetouani and B. Hammouti., 2015, Adsorption properties and inhibition of mild steel corrosion in 1 M HCl solution by some bipyrazolic derivatives: Experimental and theoretical investigations. Protection of Metals and Physical Chemistry of Surfaces 51:5, 873-884.

[22] S. John, J. Joy, M. Prajila and A. Joseph., 2011, Electrochemical, quantum chemical, and molecular

dynamics studies on the interaction of 4-amino-4H,3,5-di(methoxy)-1,2,4-triazole (ATD), BATD, and DBATD on copper metal in 1N H2SO4. Materials and Corrosion 62(11), 1031-1041.

[23] Karelson, M.; Lobanov, V.S., 1996, Quantum chemical descriptors in QSAR/QSPR studies. Chemical Reviews, 96(3), 1027-1043.

[24] Vera, L.; Guzman, M.; Ortega-Luoni, Y.P., 2006, QSPR study of corrosion inhibitors; imidazolines, Journal of the Chilean Chemical Society, 51(4), 1034-1039(2006).

[25] M. J. Frisch, G. W. Trucks, H. B. Schlegel, G. E. Scuseria, M. A. Robb, J. R. Cheeseman, G. Scalmani, V. Barone, B. Mennucci, G. A. Petersson, H. Nakatsuji, M. Caricato, X. Li, H. P. Hratchian, A. F. Izmaylov, J. Bloino, G. Zheng, J. L. Sonnenberg, M. Hada, M. Ehara, K. Toyota, R. Fukuda, J. Hasegawa, M. Ishida, T. Nakajima, Y. Honda, O. Kitao, H. Nakai, T. Vreven, J. A. Montgomery, Jr., J. E. Peralta, F. Ogliaro, M. Bearpark, J. J. Heyd, E. Brothers, K. N. Kudin, V. N. Staroverov, R. Kobayashi, J. Normand, K. Raghavachari, A. Rendell, J. C. Burant, S. S. Iyengar, J. Tomasi, M. Cossi, N. Rega, J. M. Millam, M. Klene, J. E. Knox, J. B. Cross, V. Bakken, C. Adamo, J. Jaramillo, R. Gomperts, R. E. Stratmann, O. Yazyev, A. J. Austin, R. Cammi, C. Pomelli, J. W. Ochterski, R. L. Martin, K. Morokuma, V. G. Zakrzewski, G. A. Voth, P. Salvador, J. J. Dannenberg, S. Dapprich, A. D. Daniels, Ö. Farkas, J. B. Foresman, J. V. Ortiz, J. Cioslowski and A. D. J. Fox, Gaussian, Inc., Wallingford, (2009), 09.

[26] Benhiba F., Serrar H., Hsissou R., Guenbour A., Bellaouchou A., Tabyaoui M., Boukhris S., Oudda H., Warad I. and Zarrouk A., 2020, Tetrahydropyrimido-Triazepine derivatives as anti-corrosion additives for acid corrosion: Chemical, electrochemical, surface and theoretical studies. Chemical Physics Letters 743, 137181.

[27] C. Lee, W. Yang, R.G. Parr, 1988, Development of the Colle-Salvetti correlation-energy formula into a functional of the electron density, Physical Review B, 37,785-789.

[28] Lukovits, I., Kalman, E.F., 2001, Corrosion Inhibitors — Correlation between Electronic Structure and Efficiency, Corrosion (NACE), 57(1): 3-8.

[29] J. Aljourani, K. Raessi, M. A. Golozar, 2006, Benzimidazole and its derivatives as corrosion inhibitors for mild steel in 1M HCl, Corrosion science, 51, 1836-1843.

[30] J. O'M. Bockris, D. Drazi, 1962; The kinetics of deposition and dissolution of iron: Effect of alloying impurities, Portugaliae Electrochemica Acta, 7, 293-313.

[31] M. I. Temkin, 1941, Adsorption equilibrium and process Kinetics on inhomogeneous surfaces with interaction between adsorbed molecules, Zh. Fiz. Khim, 15(3), 296-332.

[32] Y. A. El Awady, A. I. Ahmed, 1985, Effect of temperature and inhibitors on the corrosion of aluminium in 2N HCl solution, A kinetic study, Journal of Indian Chemistry, 24, 601-606.

[33] Irving Langmuir, 1916, the constitution and fundamental properties of solids and liquids, Journal of the American Chemical Society, 38(11), 2221–2295.

[34] Villamil R F. V., Corio P., Rubin J. C., Agostinho S. M. L., 1999, Effect of sodium dodecylsulfate on copper corrosion in sulfuric acid media in the absence and presence of benzotriazole, Journal of Electroanalytical Chemistry, 472, 112-116.

[35] Vashi R. T., Champaneri V. A., 1997, Toluidines as corrosion inhibitors for zinc in sulphamic acid Indian Journal of Chemical Technology, 4,180-184.

[36] Noor E.A., Al-Moubaraki A.H., 2008, Thermodynamic study of metal corrosion and inhibitor adsorption processes in mild steel/1-methyl-4[4(-X)-styryl pyridinium iodides/ hydrochloric acid systems, Materials Chemistry and Physics, 110, 145-154.

[37] F. Bentiss, M. Lebrini, M. Lagrenee, 2005, Thermodynamic characterization of metal dissolution and inhibitor adsorption processes in mild steel/2,5-bis(n-thienyl)-1,3,4-thiadiazoles/ hydrochloric acid system, Corrosion Science, 47, 2915-2931.

[38] J. D. Talati and D. K. Gandhi, 1983, N-heterocyclic compounds as corrosion inhibitors for aluminium-copper alloy in hydrochloric acid, Corrosion Science, 23(12), 1315–1332.

[39] W. Durnie, R. De Marco, A. Jefferson, and B. Kinsella, 1999, Development of a structure-activity relationship for oil field corrosion inhibitors, Journal of the Electrochemical Society, 1999, volume 146(5), 1751–1756.

[40] I.N. Putilova, S. A. Balezin, V. P. Barannik, Metallic Corrosion Inhibitors, Pergamon Press, Oxford, 1960, 30.

[41] S O Adejo; M. M Ekwenchi. IOSR., 2014, Resolution of adsorption characterisation ambiguity through the Adejo-Ekwenchi adsorption isotherm: a case study of leaf extract of Hyptis suaveolen poit as green corrosion inhibitor of corrosion of mild steel in 2 M HCl Journal of Emerging Trends in Engineering and Applied Sciences, 8(5), 201 – 205.

[42] Adejo S O; Ekwenchi M M; Ahile J U; Gbertyo J A; Kaio. A., 2014, Proposing a new empirical adsorption isotherm known as Adejo-Ekwenchi isotherm, Journal of Applied Chemistry, 6(5), 66-71.

[43] Li, Y.; Zhao, P.; Liang, Q.; Hou, B., 2005, Berberine as a natural source inhibitor for mild steel in 1 M H2SO4, Applied. Surface Science, 252(5), 1245-1253.

[44] Gomma G.K., 1998, Mechanism of corrosion behaviour of carbon steel in tartaric and malic acid in the presence of Fe2+ ion, Materials Chemistry and Physics, 52, 200-206.

[45] M. Lebrini, M. Lagrenée, H. Vezin, M. Traisnel, and F. Bentiss., 2007, Experimental and theoretical study for corrosion inhibition of mild steel in normal hydrochloric acid solution by some new macrocyclic polyether compounds. Corrosion Science, 49(5), 2254-2269.

[46] Pavithra, M. K., Venkatesha, T. V., Kumar M. K. P., and Shivayogiraju. B. S., 2013, Acalypha torta Leaf Extract as Green Corrosion Inhibitor for Mild Steel in Hydrochloric Acid Solution. Industrial & Engineering Chemistry Research., 52(2), 722-728.

[47] Koopmans T., 1934, Über T. Die Zuordnung von Wellenfunktionen und Eigenwerten zu den Einzelnen Elektronen Eines. Atoms. Physica; 1(1-6): 104–13.

[48] Parr RG, Pearson RG. 1983, Absolute hardness: companion parameter to absolute electronegativity. Journal of the American Chemical society, 105(26): 7512-7516.

[49] Parr RG, Szentpaly LL, Liu S., 1999, Electrophilicity index

Journal of the American Chemical society, 121(9): 1922-1924.

[50] Pearson RG., 1988, Absolute Electronegativity and Hardness: application to Inorganic Chemistry, Inorganic Chemistry, 27(4): 734-740.

[51] M. J. S. Dewar, E. G. Zoebisch, E. F. Healy, J. P. Stewart, 1985, Development and use of quantum mechanical molecular models, 76, AM1: a new general purpose quantum mechanical molecular model, Journal of the American Chemical Society, 107, 3902-3909.

[52] Kaya S., Kaya C., Guo L., Kandemirli F, Tüzün B., U ˘gurlu ˙I., et al., 2016, Quantum chemical and molecular dynamics simulation studies on inhibition performances of some thiazole and thiadiazole derivatives against corrosion of iron. Journal of Molecular Liquids; 219: 497–504.

[53] Tigori, M., Kouyaté, A., Kouakou, V., Niamien, P., & Trokourey, A., 2020), Computational approach for predicting the adsorption properties and inhibition of some antiretroviral drugs on copper corrosion in HNO3. European Journal of Chemistry, 11(3), 235-244.

[54] W. Yang, R.G. Parr, Hardness, softness, and the fukui function in the electronic theory of metals and catalysis. Proc. Natl. Acad. Sci. U.S.A., 1985, 82, 6723.

[55] N. Mohanapriya, M. Kumaravel and B. Lalithamani, 2020, Theoretical and Experimental Studies on the Adsorption of N- [(E)-Pyridin-2-ylmethylidene] Aniline, a Schiff Base, on Mild Steel Surface in Acid Media. Journal of Electrochemical Science and Technology 11(2), 117-131.

[56] M. Lagren´ee, B. Mernari, N. Chaibi, M. Traisnel, H. Vezin, and F. Bentiss, 2011, Investigation of the inhibitive effect of substituted oxadiazoles on the corrosion of mild steel in HCl medium, Corrosion Science, 43(5), 951–962.

[57] M. A. Quraishi and R. Sardar, 2003, Hector bases — a new class of heterocyclic corrosion inhibitors for mild steel in acid solutions, Journal of Applied Electrochemistry, 33(12), 1163–1168.

[58] K. F. Khaled, K. Babi´ c-Samard˘zija, and N. Hackerman, 2005, Theoretical study of the structural effects of polymethylene amines on corrosion inhibition of iron in acid solutions," Electrochimica Acta, 50(12), 2515–2520.

[59] Khaled, K.F., 2008, Molecular Simulation, Quantum Chemical Calculations and Electrochemical Studies for Inhibition of Mild Steel by Triazoles. Electrochimica Acta, 53(9), 3484-3492(2008).

[60] B. Gomez, N.V. Likhanova, M.A. Dominguez-Aguilar, R. Martinez-Palou, A. Vela, J.L. 2006, Gazquez, Quantum Chemical Study of the Inhibitive Properties of 2-Pyridyl-Azoles, Journal of Physical Chemistry B, 110(18), 8928–8934.

[61] G. Bereket, E. Hu¨r, and C. O¨ retir, "Quantum chemical studies on some imidazole derivatives as corrosion inhibitors for iron in acidic medium," Journal of Molecular Structure: THEOCHEM, 578(1–3), 79–88.

[62] Yang W, Mortier WJ, 1986 The use of global and local molecular parameters for the analysis of the gas-phase basicity of amines, Journal of the American Chemical Society, 108(19), 5708–5711.

[63] Mart´ınez-Araya J.I., 2015, Why the dual descriptor is a more accurate local reactivity descriptor than Fukui functions? journal of Mathematical Chemistry, 53: 451–465.

[64] Christophe Morell André Grand Alejandro Toro-Labbé, 2004, New Dual Descriptor for Chemical Reactivity. Journal of Physical Chemistry. A, 109(1): 205–212.